

MULTI-FIDELITY SEQUENTIAL BAYESIAN OPTIMIZATION AND RELIABILITY ASSESSMENT METHOD FOR THE DESIGN OF COMPLEX SYSTEMS

Romain Espoeys^{1,2}, Loïc Brevault¹, Mathieu Balesdent¹, Sophie Ricci², Paul Mycek²

¹ONERA DTIS/M2CI
Palaiseau, FRANCE

e-mail: {romain.espoeys, loic.brevault, mathieu.balesdent}@onera.fr

²CECI Cerfacs/CNRS UMR 5318
Toulouse, France

e-mail: {ricci,mycek}@cerfacs.fr

Abstract. *Solving a Reliability-Based Design Optimization (RBDO) problem is a challenging task, especially in the presence of complex systems that are modeled using computationally expensive numerical solvers. This topic has been extensively investigated in the literature. Amongst the proposed strategies, the Sequential Optimization and Reliability Assessment (SORA) method implements a decoupled resolution of the RBDO problem by sequentially iterating between deterministic optimization and reliability analysis. The idea of SORA is to solve, at each iteration, an equivalent deterministic optimization of the RBDO problem. This is achieved in a region that is considered as feasible, by shifting the constraints by a distance derived from the target failure probability. Once the deterministic optimization is performed, a reliability analysis phase is achieved by solving another optimization problem, in order to update the shifting vector for the next deterministic optimization problem. In this paper, we propose to solve the optimization problems in SORA with a Bayesian approach through an active learning strategy based on multi-fidelity surrogate models. First, the surrogate models are built in an augmented space where design variables and uncertain variables are combined. Second, the computational cost of SORA is reduced by taking advantage of lower fidelity solvers to build the surrogates. The merits of this innovative framework are demonstrated on an analytical test case as well as on a realistic test case involving the optimization of a sounding rocket subject to a probability constraint on the target altitude to reach.*

Keywords: Uncertainty Quantification, Multi-fidelity modeling, Reliability-based Design Optimization, Gaussian Process, Reliability Analysis.

1 Introduction

The design and optimization of complex systems under uncertainties often involves Reliability-Based Design Optimization (RBDO) techniques. This type of approaches involves a reliability analysis phase during the iterations of the optimization process, thus allowing for the estimation of the probability of failure of the system as the design is optimized. A design variable can, for instance, represent the diameter of a component. The design optimization is carried out as the system is constrained by a probability of failure required to be below a target threshold. Classically, uncertainties are classified into aleatory and epistemic uncertainties. In the context of RBDO, it is possible to distinguish two types of aleatory variables: the controlled uncertain variables may relate to design variables (*e.g.*, uncertainty on the diameter of a piece due to manufacturing defect) while the uncontrolled uncertain variables may reflect the stochastic effects in the system environment (*e.g.*, wind gusts).

The most naive way to solve an RBDO problem involves a nested loop approach, referred to as the two-level approach in [1], in which a reliability analysis is performed at each iteration of the optimization process. Reliability analysis requires to estimate a multidimensional integral which may involve a large number of simulation code calls. In the literature, several other approaches have been developed to solve RBDO problems in order to reduce the number of reliability analyses along the optimization process [2, 3]. These methods include single-level approaches, which rely on the rewriting of the optimization problem by integrating the reliability constraints with optimality conditions [2]. They also include decoupled approaches that consist in decoupling optimization and reliability analysis [3]. The Sequential Optimization and Reliability Assessment (SORA) method is one of the most promising decoupled approaches since it allows to converge faster to the solution of the RBDO problem by verifying the probabilistic constraints through a local, linear approximation of the constraint function boundary using a First Order Reliability Method (FORM) [4, 5]. Nevertheless, these advanced strategies still require a large number of calls to the direct code (also referred as high-fidelity code), thus remaining unaffordable for complex and accurate, yet computationally intensive solvers in industry.

A complementary reduction of the computational cost of SORA may be achieved by replacing the direct code by a surrogate model in the objective function and/or in the constraint function [6, 7, 8]. Bayesian optimization achieves the optimization of the design variables using surrogate models (*e.g.*, Gaussian Processes (GPs) [9, 10]) that are enriched with a limited number of additional calls to the high-fidelity solvers in regions of interest. These regions of interest are those of higher probability for obtaining the minimum of the objective function while satisfying the constraints. GPs have the advantage of providing the user with a prediction on the entire domain of definition and an associated confidence level in the prediction (uncertainty associated to the prediction) [11, 12]. In the literature, GPs are widely used to perform surrogate-based optimization, including RBDO [6, 7, 8]. Traditionally, surrogate models are built either in the space of design variables or in the space of uncertain variables. A framework allowing to construct the surrogate model in an *augmented space*, combining uncertain space and design space, has already been proposed in [7, 13] as a means to save and reuse information along the iterations and improve the process of optimization under uncertainty. However, in the context of Bayesian RBDO, as this approach leads to a possibly significant increase of the dimension of the input space, many calls to the high-fidelity code may be required to obtain an accurate surrogate model, thus making it computationally expensive.

One way to reduce the cost for the construction of the surrogate model is to aggregate mul-

multiple sources of information, with the use of lower-fidelity models. These solvers with different fidelities are used to build multi-fidelity surrogate models for the RBDO strategy. Low-fidelity models are less expensive and less accurate than the high-fidelity solver, thus introducing additional modeling uncertainties. For example, the aerodynamic simulation of an aerospace vehicle can be carried out with a CFD RANS (Computational Fluid Dynamics, Reynolds Averaged Navier-Stokes) code (high fidelity), or with an Euler-type CFD code (low fidelity, simplifications on viscosity). RANS calculations present a higher prediction accuracy than Euler calculations but for a larger computational cost. Several multi-fidelity techniques have been investigated based on GPs [14, 15, 16]. The most common method is the Auto-Regressive Model (AR1 [15]), which is appropriate when the outputs of low-fidelity and high-fidelity codes present linear dependencies [17]. The description of both aleatory and epistemic uncertainties that relate to the accuracy of the different fidelities of the surrogate models should be carefully taken into account in the workflow of multi-fidelity RBDO. This is a challenging task and an active field of research [18, 19, 20, 21].

This article proposes a modified SORA method, named MFB-SORA for Multi-Fidelity Bayesian SORA. This strategy is based on three different contributions. It mainly consists in coupling the SORA framework with *Bayesian optimization*, taking advantage of the benefits of SORA while minimizing the overall calculation cost of the method by using surrogate models. In addition, a framework for reusing surrogate information throughout the optimization process based on the *augmented space* is adopted. Surrogate models are enriched all along the SORA process in the joint space combining design and uncertain variables. Finally, in order to take advantage of multiple sources of information, *multi-fidelity* surrogate models are built and enriched during the Bayesian optimization in the augmented space to reduce the global computational cost of the SORA method.

This paper is organized as follows. Section 2 introduces a brief state of the art of RBDO techniques and multi-fidelity optimization approaches. Section 2.1 presents the formulation of the RBDO problem and several techniques to solve it, as well as the augmented space formulation. Then, Section 2.2 presents multi-fidelity Bayesian optimization. Section 3 presents the proposed SORA approach based on multi-fidelity Bayesian optimization in the augmented space. The approach presented in this paper is compared with other approaches reported in the literature, such as double-loop and standard SORA. They are assessed on different test cases in Section 4. The first case is an analytical test case and the second is an aerospace test case of greater complexity with multidisciplinary simulation models for the optimization of a sounding rocket considering different uncertainties. Perspectives and conclusion are presented in Section 5.

2 State of the Art

The following brief state of the art introduces the main bricks for the Multi-fidelity Bayesian RBDO approach. First, the existing RBDO formulations are described with a focus on SORA. Then, the concept of augmented space defining a joint domain combining the design variables and the uncertain variables is presented. Eventually, multi-fidelity Bayesian optimization is briefly presented in order to efficiently solve an optimization problem when different fidelity models are available.

2.1 Reliability-Based Design Optimization (RBDO)

2.1.1 Problem formulation

An RBDO problem [22] is an optimization problem under uncertainty. There are different ways to formulate such a problem. In the present paper, the chosen formulation is derived from works presented in [3, 20]. The objective function of the RBDO problem is assumed to be deterministic and depends on the value of deterministic vectors \mathbf{d} of size n_d and \mathbf{p} of size n_p . The variables \mathbf{d} are classical design variables and the variables \mathbf{p} correspond to some hyperparameters associated to the aleatory variables \mathbf{X} . Consider for instance the mass of propellant to optimize, while the final mass is uncertain due to uncertainty during the fueling operation before launch. The propellant mass can be represented as the Gaussian variable $\mathbf{X} \sim \mathcal{N}(\mathbf{p}, \sigma^2)$ with a mean \mathbf{p} that is optimized corresponding to the target specification and a certain variance σ^2 related to fueling operation.

The random variables representing the aleatory parameters of the problem may be of different nature. They may be *controlled* because they are linked to an optimization parameter or *uncontrolled*. The former will be represented by \mathbf{X} , and parameterized by \mathbf{p} , as described above, with a corresponding probability density function (PDF) $\phi_{\mathbf{X}|\mathbf{p}}$. The latter will be denoted by \mathbf{Z} , with a corresponding PDF $\phi_{\mathbf{Z}}$. The sizes of the random vectors \mathbf{X} and \mathbf{Z} are respectively n_X and n_Z . In the optimization problem, it is possible to consider deterministic constraints. In addition, the presence of uncertainties leads to the presence of probabilistic constraints, *i.e.*, involving a constraint function $g(\cdot)$ subject to aleatory variables describing the uncertainties of the system, and/or design variables. In the following, it is assumed that the system failure occurs when the function $g(\cdot)$ is negative. In this work, probabilistic constraints are modeled by failure probabilities with an associated target failure probability not to be exceeded (denoted by P_f^t), *i.e.* $\mathbb{P}[g(\mathbf{d}, \mathbf{X}(\mathbf{p}), \mathbf{Z}) \leq 0] \leq P_f^t$. For the sake of simplicity, and because the study deals with optimization under probabilistic constraints, deterministic constraints will not appear in the formulation of the problem to be solved. The corresponding RBDO problem thus reads

$$\min_{\mathbf{d}, \mathbf{p}} f(\mathbf{d}, \mathbf{p}) \quad \text{s.t.} \quad \begin{cases} \mathbb{P}[g_i(\mathbf{d}, \mathbf{X}(\mathbf{p}), \mathbf{Z}) \leq 0] \leq P_{f,i}^t & \text{for } i = 1, \dots, n_g \\ \mathbf{d}^- \leq \mathbf{d} \leq \mathbf{d}^+ \\ \mathbf{p}^- \leq \mathbf{p} \leq \mathbf{p}^+ \end{cases} \quad (1)$$

where $f(\cdot)$ is the objective function to be minimized. It is assumed that $f(\cdot)$ depends on the deterministic parameters \mathbf{d} and \mathbf{p} , defined in the optimization domain $[\mathbf{d}^-, \mathbf{d}^+]$ and $[\mathbf{p}^-, \mathbf{p}^+]$, and is subjected to the n_g constraints involving $g_i(\cdot)$ that are, in turn, dependent to the parameters \mathbf{d} as well as to the uncertain parameters \mathbf{X} and \mathbf{Z} . In this formulation, $P_{f,i}^t$ represents the target maximal failure probability of the i^{th} probabilistic constraint.

2.1.2 RBDO approaches

Several techniques for solving RBDO problems have been proposed in the literature [7, 22]. The difficulty in RBDO is that at each iteration of the optimization process, a calculation of the probability of failure of each constraint must be performed. In order to solve such an optimization problem in practice, different types of methods have emerged, as shown in Figure 1: the *two-level approaches* [1], the *single-level approaches* [2] and the *decoupled approaches* [3].

The first and most direct technique to solve an RBDO problem is the *two-level approach*. It leads to a reliability analysis problem nested in an optimization one, where the outer loop solves the minimization problem, while the probability of failure of each probabilistic constraint

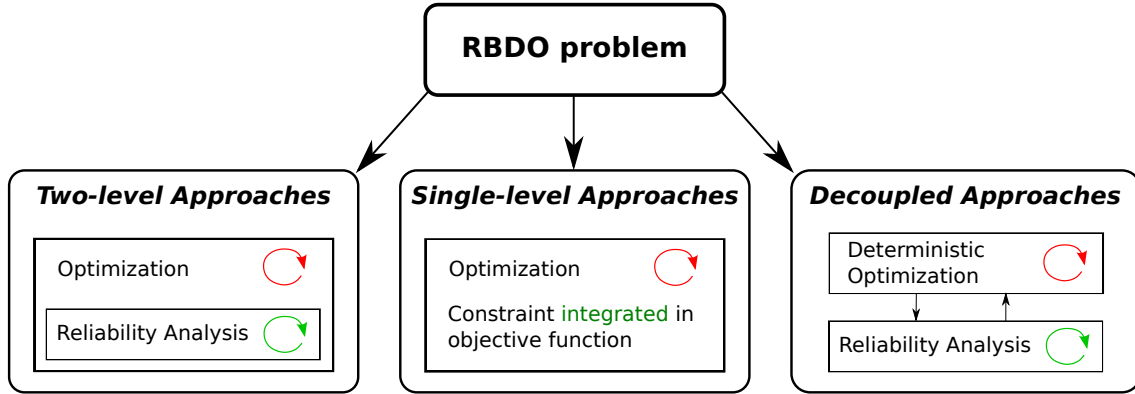


Figure 1: Classification of RBDO techniques

is estimated at each iteration of the optimization. An intuitive but expensive way to solve the reliability analysis is to calculate each probability of failure with a Monte-Carlo sampling [23]. A more efficient probability estimation has been proposed by Nikolaidis and Burdisso [24]. They developed the reliability index approach (RIA) using the First Order Reliability Method (FORM) [4, 5], which allows for the analytical calculation of the probability of failure via a linear approximation of the limit state function at the Most Probable Failure Point (MPFP). In order to find the MPFP, an auxiliary optimization problem involving the constraint function $g_i(\cdot)$, is solved. In their research work, Tu *et al.* [1] proposed an alternative two-level approach called Performance Measure Approach (PMA) which consists of an inverse reliability problem (using an inverse FORM [25]), based on the search of the point with minimum performance that remains consistent with a target probability; the Minimum Performance Target Point (MPTP). Indeed, the auxiliary optimization problem to find MPTP is easier to solve than the one to find the MPFP.

Alternatively to two-level approaches, *single-level approaches* (or *single-loop approaches*) consist in reformulating the RBDO problem as a problem without direct reliability analysis. The probabilistic constraints are replaced by equivalent optimal conditions (for instance based on Karush Kuhn Tucker optimality conditions [26]). The goal is then to solve this new deterministic optimization problem in a single-loop procedure that minimizes the objective function while respecting the constraints. Based on this idea, Liang *et al.* developed the Single Loop Approach [2].

Finally, the *decoupled approach* aims at decoupling the optimization part from the reliability assessment. This concept is devised in the SORA method introduced by Du and Chen [3]. This technique sequentially solves a deterministic optimization (DO) problem and a reliability assessment (RA) via an inverse FORM technique. For that purpose, the probabilistic constraints are replaced by equivalent deterministic constraints shifted by a certain distance consistent with the desired acceptable failure probability P_f^t . The key idea is to solve the deterministic optimization problem in a region considered as feasible with respect to the probabilistic constraints. The shifting vector is updated at each sequential loop iteration via the MPTP update (inverse FORM reliability analysis loop).

Despite the efficiency of these alternative techniques as compared to double-loop approaches, the costs of high-fidelity codes may render them unaffordable for complex industrial problems. In order to lower the computational cost of RBDO problem, *Surrogate-based approaches* have been developed [6, 7, 8]. The key idea is to replace the objective and constraint functions by surrogate models built from a database of simulations. These approaches have been coupled

with the the different categories of RBDO formulations presented above.

2.1.3 The Sequential Optimization and Reliability Assessment (SORA) method

As previously stated, the RBDO approach in the present paper is based on SORA. We detail here the general framework of this method. The problem to solve is defined by Eq. (1). The sequential loop starts by initializing the shifting vector to zero and the random vector \mathbf{Z} to its mean value \mathbf{m}_Z . Then, a deterministic optimization problem is solved. Here, each probabilistic constraint is replaced by an equivalent deterministic shifted constraint. During this optimization process, the uncertain variables \mathbf{Z} are fixed at the MPTP, *i.e.*, at their critical values consistent with the target failure probability P_f^t (or at their mean value for the first iteration of SORA) and the uncertain variables \mathbf{X} are shifted with the shifting vector. At the k^{th} sequential step of SORA, the deterministic optimization problem is therefore defined as

$$\mathbf{d}_*^{(k)}, \mathbf{p}_*^{(k)} = \arg \min_{\mathbf{d}, \mathbf{p}} f(\mathbf{d}, \mathbf{p}) \quad \text{s.t.} \quad \begin{cases} g_i(\mathbf{d}, \mathbf{p} - \mathbf{s}_i^{(k)}, \mathbf{Z}_{\text{MPTP},i}^{(k)}) \geq 0 & \text{for } i = 1, \dots, n_g \\ \mathbf{d}^- \leq \mathbf{d} \leq \mathbf{d}^+ \\ \mathbf{p}^- \leq \mathbf{p} \leq \mathbf{p}^+ \end{cases} \quad (2)$$

where $\mathbf{s}_i^{(k)}$ is the shifting vector and $\mathbf{Z}_{\text{MPTP},i}^{(k)}$ the MPTP of the random vector \mathbf{Z} related to the constraint function $g_i(\cdot)$. The pair $\{\mathbf{d}_*^{(k)}, \mathbf{p}_*^{(k)}\}$ is the solution of the deterministic optimization problem at iteration k .

Then, following the deterministic optimization phase, a reliability analysis is carried out with the design vector \mathbf{d} and the parameter vector \mathbf{p} fixed at their respective optimal value $\mathbf{d}_*^{(k)}$ and $\mathbf{p}_*^{(k)}$ from the previous step. The reliability analysis amounts to solving an optimization problem which involves an inverse FORM to determine the MPTP. This search of the MPTP stands in the following optimization problem:

$$\mathbf{u}_i^* = \arg \min_{\mathbf{u}} G_i(\mathbf{d}_*^{(k)}, \mathbf{u}) \quad \text{s.t.} \quad \|\mathbf{u}\| = \beta_i^t \quad \text{for } i = 1, \dots, n_g \quad (3)$$

where $\mathbf{d}_*^{(k)}$ is the optimal design parameter \mathbf{d} of the k^{th} deterministic optimization, $G_i(\mathbf{d}, \mathbf{u}) = g_i(\mathbf{d}, \mathcal{T}_{p_*^{(k)}}^{-1}(\mathbf{u}))$, with $\mathcal{T}_{p_*^{(k)}}(\cdot)$ the appropriate iso-probabilistic transformation parameterized by the aleatory variables (\mathbf{X} and \mathbf{Z}) at the solution point $\mathbf{p}_*^{(k)}$, and $\mathbf{u} = \mathcal{T}_{p_*^{(k)}}\{\mathbf{X}, \mathbf{Z}\}$. The target distance β_i^t is related to $P_{f,i}^t$ by $\beta_i^t = -\Phi^{-1}(P_{f,i}^t)$, where Φ is the cumulative density function (CDF) of the normal distribution. The solution given by the inverse FORM procedure is then $\{\mathbf{X}_{\text{MPTP},i}^{(k)}, \mathbf{Z}_{\text{MPTP},i}^{(k)}\} = \mathcal{T}_{p_*^{(k)}}^{-1}(\mathbf{u}_i^*)$. The MPTP value of the random vector \mathbf{Z} is updated for the next DO, and the shifting vector becomes

$$\mathbf{s}_i^{(k+1)} = \mathbf{p}_*^{(k)} - \mathbf{X}_{\text{MPTP},i}^{(k)} \quad (4)$$

The SORA method iterates equations Eq. 2, Eq. 3 and Eq. 4, as shown in Fig. 2 until a stopping criterion is reached. At the convergence, the shifting vector as well as the DO solution should stabilise.

In the literature, the SORA approach have been coupled with surrogate models. For instance, a modified version of SORA have been introduced by Song *et al.* [20]. It proposes to build and enrich the surrogate models of the objective function and the constraint functions by active

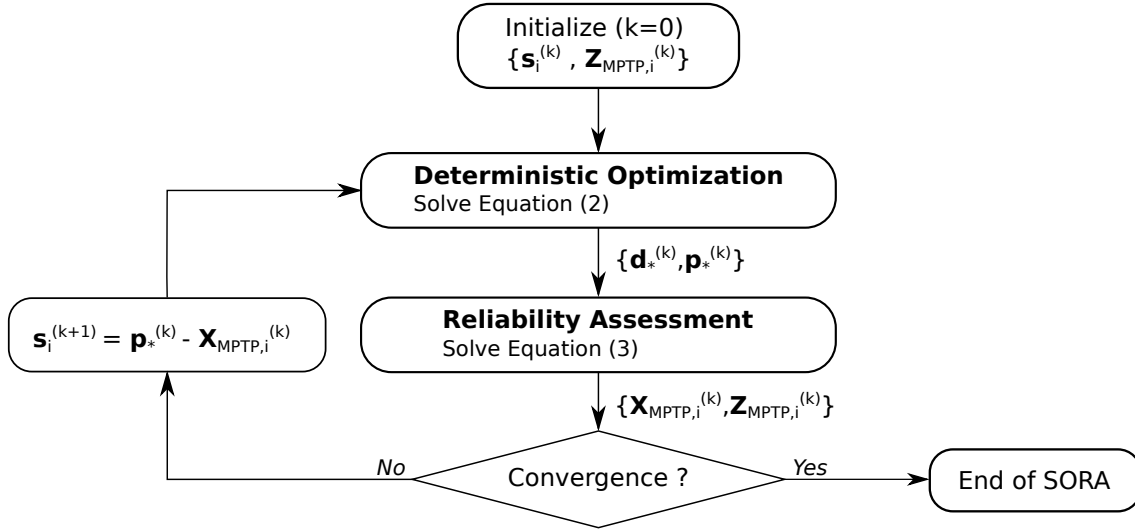


Figure 2: Flowchart of SORA method

learning, and then replace the exact functions in SORA by the corresponding surrogate models, thus allowing for a considerable reduction of the computational cost of both the optimization and reliability steps. However, some limitations for this approach should be stated. Indeed, the surrogates are built upstream of the RBDO problem, so the enrichment is not guided by the optimization problem nor by the reliability analysis. In addition, the enrichment of the GP over the entire input space means that the surrogate is not particularly accurate and reliable around the optimum. It might also lead to some unnecessary high fidelity model evaluations in regions of poor interest with respect to optimization or reliability analysis.

2.1.4 Augmented Space framework for surrogate-based RBDO techniques

As previously stated, surrogate-based techniques aim at reducing the computational cost of RBDO. The description of the domain of definition for the surrogate model is of prime importance especially in the context of RBDO with the presence of the design space and uncertain space (with some possible interaction via the distribution parameters of the uncertain variables that can be considered as optimization variables). In Eq. (1), the objective function depends on deterministic parameters while the constraints depend on both deterministic parameters (the design variables) and uncertain parameters (the random variables).

Building the surrogates for the constraint functions $g_i(\mathbf{X}, \mathbf{Z} | \mathbf{d}_*^{(k)}, \mathbf{p}_*^{(k)})$, with respect to the current value of $\mathbf{d}_*^{(k)}$ and $\mathbf{p}_*^{(k)}$, at each iteration of the optimization process, prevents from reusing the surrogate between iterations as the domain of definition may change. Alternatively, building the surrogate in an *augmented space* alleviates this limitation. Au [13] proposed to define a new joint input space for the definition of the surrogate model that spans both the design variables and the uncertain variables. More details on the construction of the *augmented space* are found in [7].

In Eq. (1), the probabilistic constraints depend on the design vector \mathbf{d} , the random vector \mathbf{X} following a PDF parameterized by the vector parameter \mathbf{p} , and the random vector \mathbf{Z} . The construction of the augmented space is thus defined as the tensor product of the “confidence region” of each variable, corresponding to the region in which the surrogate model is built in order to avoid extrapolation difficulties.

The confidence region \mathbb{D} , for the design variables \mathbf{d} , is defined by its deterministic bounds:

$$\mathbb{D} = \bigtimes_{i=1}^{n_d} [d_i^-, d_i^+]. \quad (5)$$

We now define the corresponding confidence regions \mathbb{X} and \mathbb{Z} for each random vector \mathbf{X} and \mathbf{Z} . The random vector \mathbf{X} is parameterized by the design variables $\mathbf{p} \in [\mathbf{p}^-, \mathbf{p}^+]$. For such a vector, the confidence region is defined according to the probability of sampling outside the constructed area noted α_X , at the lower and upper bounds p_j^- and p_j^+ , for $j = 1, \dots, n_p$ (in the case where \mathbf{p} is the mean of \mathbf{X}). These probabilities are defined such that $x_j^- = \mathcal{F}_{X_j|p_j^-}^{-1}(\alpha_X)$ and $x_j^+ = \mathcal{F}_{X_j|p_j^+}^{-1}(1 - \alpha_X)$, where $\mathcal{F}_{X_j|p_j^-}^{-1}$ and $\mathcal{F}_{X_j|p_j^+}^{-1}$ are the inverse CDF of X_j at the lower and upper bounds p_j^- and p_j^+ , respectively. The corresponding confidence region thus reads

$$\mathbb{X} = \bigtimes_{j=1}^{n_p} [x_j^-, x_j^+], \quad (6)$$

As before, let us define the probability α_Z of sampling outside the area for the variable Z . The lower and upper bounds are defined symmetrically around its mean, such that $z_k^- = \mathcal{F}_{Z_k}^{-1}(\alpha_Z)$ and $z_k^+ = \mathcal{F}_{Z_k}^{-1}(1 - \alpha_Z)$. The corresponding confidence region reads

$$\mathbb{Z} = \bigtimes_{k=1}^{n_z} [z_k^-, z_k^+]. \quad (7)$$

Finally, the augmented space \mathbb{S} is constructed by a Cartesian product of the marginal confidence regions of each variable $\mathbb{S} = \mathbb{D} \times \mathbb{X} \times \mathbb{Z}$.

This approach allows to make the most of the information learnt during both optimization and reliability analysis. Yet, the large dimension of the augmented input space may prevent from building an accurate surrogate in the presence of expensive solvers, thus leading to a sub-optimal solution. Multi-fidelity techniques might then be considered provided that lower fidelity models are available. Then, both the high-fidelity model and the lower fidelity models may be evaluated to build surrogate models of the objective and constraint functions in the RBDO strategy, at a reduced overall computational cost.

In the next paragraph, multi-fidelity surrogate construction techniques are briefly introduced.

2.2 Multi-fidelity Bayesian Optimization

2.2.1 Description of Auto-Regressive models

Multi-fidelity approaches based on GPs have been extensively documented in the literature [14, 15, 16]. Among them, the Auto-Regressive (AR1) approach [15] is one of the most popular ones thanks to its simplicity of implementation. AR1 is based on the hypothesis of linear dependency between two consecutive levels of fidelity. Each level of fidelity t is replaced by a GP and a linear relationship is prescribed between two successive GPs. AR1 has been chosen for the MFB-SORA algorithm in the present work, without loss of generality. Indeed, other multi-fidelity approaches could be used depending on the assumption regarding the relationship between the different fidelities.

For each GP $f_t(\cdot)$ corresponding to the level of fidelity t (with $t \in [1, \dots, n_l]$), the prior mean function is often assumed to be constant and a covariance function $k_t(\cdot, \cdot)$ is chosen. The linear dependency between GPs reads $f_t(\mathbf{x}) = \rho_{t-1}(\mathbf{x})f_{t-1}(\mathbf{x}) + \gamma_t(\mathbf{x})$, where $\gamma_t(\cdot)$ is a GP

corrector with prior mean μ_{γ_t} , independent of $f_{t-1}(\cdot)$. The scaling function $\rho_{t-1}(\cdot)$ represents the linear correlation between two successive fidelities t and $t-1$. In practice, this factor is often assumed to be constant, and is an additional hyperparameter to be learnt. The hyperparameters of the n_l GPs of the problem are learnt at once within a large optimization problem. Considering a constant scaling factor, the formulation of the GP reads

$$f_t(\mathbf{x}) = \rho_{t-1}f_{t-1}(\mathbf{x}) + \gamma_t(\mathbf{x}). \quad (8)$$

An alternative training approach is proposed by Le Gratiet and Garnier [27] where GPs are trained sequentially under the assumption of nested training DoEs for the different fidelities. This recursive construction allows to avoid too large optimization problem when the n_l are learnt simultaneously. In the recursive construction, the GP prior $f_{t-1}(\cdot)$ in Eq. (8) is replaced by the GP posterior $f_{t-1}^*(\cdot)$. With this formulation, at the level t , the hyperparameters to learnt are the ones of the GP corrector and the scaling factor ρ_{t-1} . Once the multi-fidelity GP has been trained, the predictive mean $\mu_t^*(\cdot)$ and variance $\sigma_t^{*2}(\cdot)$ for each level t are defined by

$$\mu_t^*(\mathbf{x}) = \rho_{t-1}\mu_{t-1}^*(\mathbf{x}) + \mu_{\gamma_t}^* + k_{\mathbf{x}M_t}K_t^{-1}(\mathcal{Y}_t - \rho_{t-1}\mu_{t-1}^*(\mathcal{X}_t) - \mu_{\gamma_t}^*), \quad (9)$$

$$\sigma_t^{*2}(\mathbf{x}) = \rho_{t-1}\sigma_{t-1}^{*2}(\mathbf{x}) + k_{\mathbf{x},\mathbf{x}} - k_{\mathbf{x}M_t}K_t^{-1}k_{\mathbf{x}M_t}^T, \quad (10)$$

where M_t is the number of data at level t , K_t^{-1} is the block of the covariance matrix corresponding to the DoE $\{\mathcal{X}_t, \mathcal{Y}_t\}$ at fidelity t with $\mathcal{X}_t = [\mathbf{x}_t^1, \dots, \mathbf{x}_t^{M_t}]$, \mathbf{x}_t^i is the i^{th} data point of the DoE at fidelity t , $k_{\mathbf{x}M_t} = [k(\mathbf{x}, \mathbf{x}_t^1), \dots, k(\mathbf{x}, \mathbf{x}_t^{M_t})]$, and $\mu_{\gamma_t}^*$ is the posterior mean of $\gamma_t(\cdot)$.

As previously stated, we propose to combine a multi-fidelity Bayesian optimization approach with the SORA procedure. Now that the construction of the GP surrogates for the different fidelities has been detailed, the following parts introduce Bayesian optimization and how it integrates multi-fidelity.

2.2.2 Bayesian Optimization (BO) approach

Classical BO approaches are based on active learning strategies [28] in which a surrogate model is enriched. Let us consider the following constrained optimization problem:

$$\min_{\mathbf{x} \in \mathcal{X}} f(\mathbf{x}) \quad \text{s.t.} \quad g(\mathbf{x}) \geq 0 \quad (11)$$

where $f(\cdot)$ is the objective function and $g(\cdot)$ is the constraint function, both depending on \mathbf{x} , defined on \mathcal{X} .

The surrogate models for $f(\cdot)$ and $g(\cdot)$ are constructed and enriched from a limited DoE. The enrichment of the DoEs should improve the prediction of the surrogates in the areas of interest along the optimization process in the purpose of targeting the global minimum of the objective function while satisfying the constraint. The enrichment process results from solving an auxiliary optimization problem of maximizing an acquisition function. It is chosen to work with two acquisition function that will be coupled, one to target the global optimum of the problem and one for the constraint handling. In the context of unconstrained optimization, the *probability of improvement* (PI) [29, 30], the *expected improvement* (EI) [28] and the *lower confidence bound* (LCB) [31, 32] are popular examples of acquisition functions for DoE enrichment. A new point is selected by minimizing (or maximizing) the chosen acquisition function, and then is evaluated on the exact objective function $f(\cdot)$. The LCB acquisition function has the advantage of

providing each iteration with the solution of the optimization problem (based on surrogates and considering the variance prediction associated to the multi-fidelity GPs). Due to the important exploration component of EI, stopping criterion of the entire SORA process might be difficult to define compared to LCB enrichment criterion. In the following, it is chosen to use the LCB function without loss of generality for the proposed framework. It is defined as follows:

$$\text{LCB}(\mathbf{x}) = \mu_f(\mathbf{x}) - \alpha * \sigma_f(\mathbf{x}), \quad (12)$$

where $\mu_f(\cdot)$ and $\sigma_f^2(\cdot)$ represent the predictive mean and variance of the objective function f at the point \mathbf{x} , and the parameter α is a scalar parameter specifying the exploitation/exploration balance.

In a constrained optimization context, specific functions have been developed in order to exploit the information of the surrogate model of $g(\cdot)$, such as the *probability of feasibility* (PF) [33] or the *expected violation* (EV) [34]. In the following, we shall use the EV function without loss of generality for the proposed method. The idea of EV is to use the prediction of the surrogate of the constraint and its associated uncertainty to evaluate the risk of violation of the exact constraint function. The EV is defined as

$$\text{EV}(\mathbf{x}) = -\mu_g(\mathbf{x}) * \Phi\left(\frac{-\mu_g(\mathbf{x})}{\sigma_g}\right) + \sigma_g(\mathbf{x}) * \phi\left(\frac{-\mu_g(\mathbf{x})}{\sigma_g}\right), \quad (13)$$

where $\Phi(\cdot)$ and $\phi(\cdot)$ are respectively the CDF and the PDF of the normal distribution, and $\mu_g(\cdot)$ and $\sigma_g^2(\cdot)$ denote the predictive mean and variance of the GP of the constraint function. Finally, the new point to enrich the DoEs is chosen such that

$$\mathbf{x}^{\text{new}} = \arg \min_{\mathbf{x} \in \mathcal{X}} \text{LCB}(\mathbf{x}) \quad \text{s.t.} \quad \text{EV}(\mathbf{x}) \leq T \quad (14)$$

where T is a threshold corresponding to the maximum accepted constraint violation.

When models of different fidelities are available, the BO acquisition function must be adapted in order to solve the optimization problem efficiently. In the following, BO with multi-fidelity is presented.

2.2.3 Multi-fidelity Bayesian Optimization (MFBO)

In order to enrich the multi-fidelity surrogate model along the BO process, in addition to the location of the new point to be added to the DoE, it is necessary to determine which level of fidelity will be used to evaluate the point selected.

Different strategies have been proposed in the literature [35, 36, 37, 38, 39, 40]. A possible approach is to solve Eq. (14) with the LCB function defined using the prediction mean and variance of the higher-fidelity GP. Let $\text{LCB}(t, \mathbf{x})$ and $\text{EV}(t, \mathbf{x})$ denote the LCB acquisition function and the EV function computed at \mathbf{x} with the surrogate predictions for fidelity t . Then, a fidelity selection criterion is used to select the level of fidelity t^{new} of the model to be evaluated at the new chosen point \mathbf{x}^{new} . In their paper, Meliani *et al.* [41] developed a criterion based on the variance reduction $\sigma_{\text{red}}^2(t, \mathbf{x}^{\text{new}})$ resulting from adding the point \mathbf{x}^{new} at fidelity level t , weighted by the cost of each fidelity, defined as

$$\sigma_{\text{red}}^2(t, \mathbf{x}^{\text{new}}) = \sum_{i=1}^t \sigma_{\gamma,i}^2(\mathbf{x}^{\text{new}}) \prod_{j=i}^{n_t-1} \rho_j^2, \quad (15)$$

where $\sigma_{\gamma,i}^2$ and ρ_j are respectively the variance of the GP corrector at fidelity i and the scaling factor in Eq. (8). Finally, the pair $\{\mathbf{x}^{\text{new}}, t^{\text{new}}\}$ is selected by solving

$$\begin{cases} \mathbf{x}^{\text{new}} = \arg \min_{\mathbf{x} \in \mathcal{X}} \text{LCB}(n_l, \mathbf{x}) & \text{s.t. } \text{EV}(n_l, \mathbf{x}) \leq T \\ t^{\text{new}} = \arg \max_{t \in \{1, \dots, n_l\}} \frac{\sigma_{\text{red}}^2(t, \mathbf{x}^{\text{new}})}{\text{cost}_{\text{total}}(t)^2} \end{cases} \quad (16)$$

where n_l corresponds to the highest level of fidelity, $\text{cost}_{\text{total}}(t) = \sum_{i=1}^t c_i$, with c_i the cost of fidelity level i .

The major concepts have been summarized in this section. They are now combined in the Multi-fidelity Bayesian SORA approach, as detailed in the following section.

3 Multi-fidelity Bayesian Sequential Optimization and Reliability Assessment (MFB-SORA) Method

3.1 Proposed method framework

Similarly to the standard SORA approach, the optimization problem is formulated as a sequence of two optimization problems: deterministic optimization (DO) and reliability analysis (RA). In the present work, the SORA method is modified so that both the deterministic optimization and the reliability analysis (Eq. (2) and Eq. (3)) are solved using multi-fidelity BO. This allows to benefit from the computational efficiency and robustness of BO methods. In practice, multi-fidelity surrogate models of the objective function $f(\cdot)$ and of the constraint functions $g_i(\cdot)$ are constructed and enriched all along the SORA procedure. This strategy limits the evaluation of the exact objective and constraint functions to the regions of interest with respect to the optimization problem and the reliability analysis. Moreover, the construction of the surrogate model of $g_i(\cdot)$ in the augmented space allows to exploit the data from previous iterations of the SORA procedure, so that fewer and fewer evaluations of the exact objective and constraint functions should be required as the SORA iterations progress. With this approach, the respective DoEs for the objective and constraint functions are enriched throughout the SORA process, thus improving the accuracy of the surrogate prediction.

Figure 3 presents the MFB-SORA flowchart devised with the multi-fidelity BO and the enrichment strategies for the multi-fidelity DoEs in the bi-fidelity case ($t \in \{\text{LF}, \text{HF}\}$). Here, $\{\mathcal{X}_{f,t}^{(k)}, \mathcal{Y}_{f,t}^{(k)}\}$ and $\{\mathcal{X}_{g_i,t}^{(k)}, \mathcal{Y}_{g_i,t}^{(k)}\}$ are respectively the DoEs for the objective function $f(\cdot)$ and constraint functions $g_i(\cdot)$ at fidelity level t , and iteration k of SORA. The lay out of the modified SORA procedure applied to RBDO problem Eq. (1) is displayed in Algorithm 1.

When AR1 is used, the multi-fidelity DoEs should be nested. The DoEs of each fidelity of $f(\cdot)$ are enriched during the DO cycles. Similarly, the DoEs of each constraint function $g_i(\cdot)$ are enriched with the same points during the DO phase. Then, the constraint functions $g_i(\cdot)$ become the objective function for the optimization problem Eq. (3) for the RA phase. The DoEs of $g_i(\cdot)$ are then enriched during RA. Since the surrogate of $g_i(\cdot)$ is constructed in the augmented space, its multi-fidelity DoE must be enriched in this space. Indeed, during the DO, the DoE of $g_i(\cdot)$ is enriched with respect to the deterministic parameters (shifted by $\mathbf{s}_i^{(k)}$) while the uncertain variables are fixed. During the RA, the DoE of $g_i(\cdot)$ is enriched with respect to the uncertain variables while the design variables are fixed. Furthermore, as the AR1 formulation is used, when a data point is added to a high-fidelity DoE, it should also be added to the lower-fidelity ones in order to respect the nesting assumption. Enrichment strategies are detailed in sections

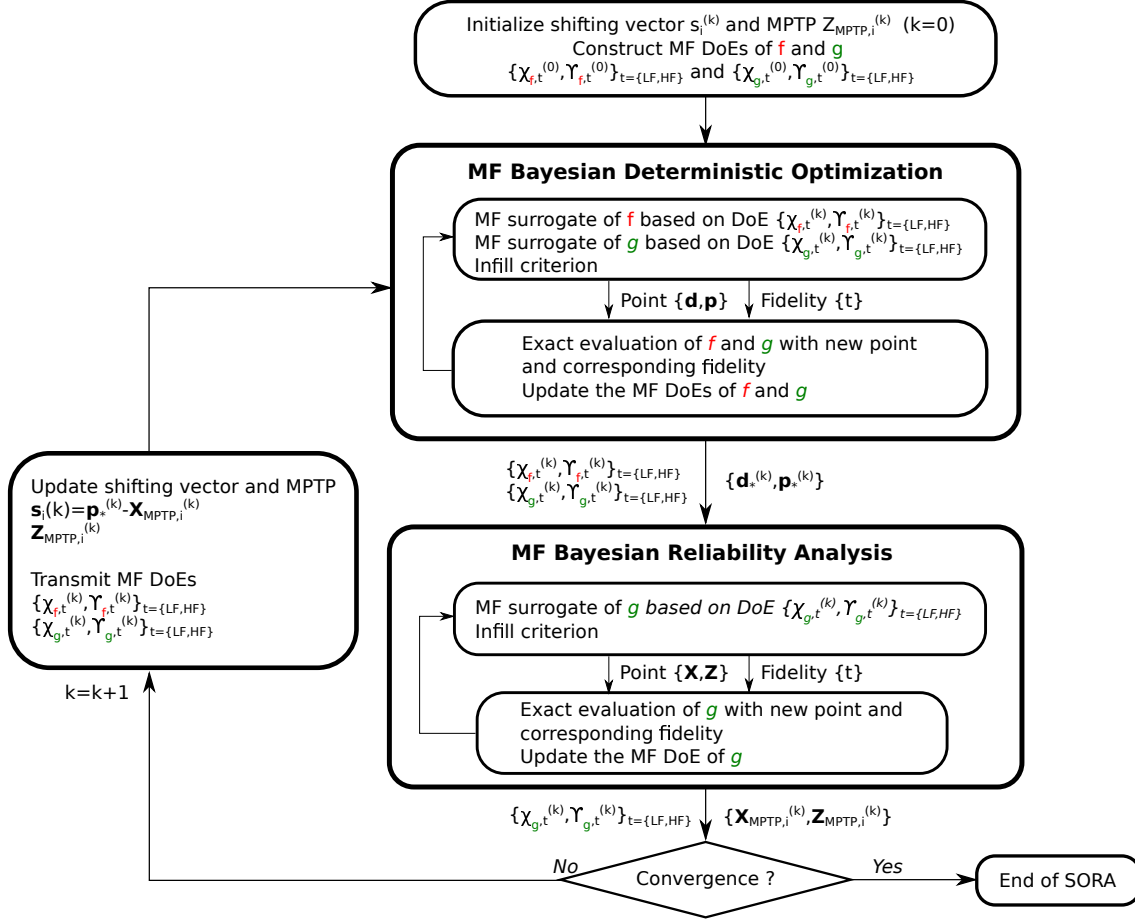


Figure 3: Flowchart of the proposed MFB-SORA method.

3.2 and 3.3.

3.2 Multi-fidelity Bayesian Optimization for Deterministic Optimization

The first optimization sub-problem to treat is the one in Eq. (2). The strategy to solve this problem is the same as presented in Section 2.2.3. First, a limited DoE is selected and enriched using the LCB acquisition function. The respect of constraints are handled by the EV function, which has the advantage of targeting the area where the constraints are violated, based on the GP prediction and its associated variance. This allows to directly control the tolerated violation for each constraint. In the DO phase of the proposed SORA approach, the location of the new point is selected such that

$$\mathbf{q}_{DO}^{new} = \arg \min_{\mathbf{q}} \text{LCB}_f(n_l, \mathbf{q}) \quad \text{s.t.} \quad \text{EV}_{g_i}(n_l, \mathbf{q}_{\text{shifted}}) < T_i \quad \text{for } i = 1, \dots, n_g \quad (17)$$

where $\mathbf{q} = \{\mathbf{d}, \mathbf{p}\}$ is the vector of the design variables, $\text{LCB}_f(n_l, \mathbf{q})$ denotes the LCB for the high-fidelity ($t = n_l$) surrogate prediction of $f(\cdot)$ at the point \mathbf{q} , and $\text{EV}_{g_i}(n_l, \mathbf{q})$ denotes the expected violation for the high-fidelity ($t = n_l$) surrogate prediction of $g_i(\cdot)$ at the point $\mathbf{q}_{\text{shifted}} = \{\mathbf{d}, \mathbf{p} - \mathbf{s}_i^{(k)}\}$. The vector $\mathbf{s}_i^{(k)}$ denotes the current shifting vector for constraint $g_i(\cdot)$.

Then, the level of fidelity is selected as in Eq. (16),

Algorithm 1 MFB-SORA algorithm for two level of fidelities denoted LF and HF for Low Fidelity and High Fidelity respectively.

$k \leftarrow 0$ ▷ SORA loop counter
 $\mathbf{s}_i^{(k)} \leftarrow \mathbf{0}$, for $i = 1, \dots, n_g$
 $\mathbf{Z}_{\text{MPTP},i}^{(k)} \leftarrow \mathbf{m}_Z$, for $i = 1, \dots, n_g$
 $\{\mathcal{X}_{f,t}^{(k)}, \mathcal{Y}_{f,t}^{(k)}\}_{t=\{\text{LF},\text{HF}\}}$
 $\{\mathcal{X}_{g_i,t}^{(k)}, \mathcal{Y}_{g_i,t}^{(k)}\}_{t=\{\text{LF},\text{HF}\}}$ (for $i = 1, \dots, n_g$)
while (stopping criterion not reached) **do**
 ### DO phase
 Inputs: $\{\mathcal{X}_{f,t}^{(k)}, \mathcal{Y}_{f,t}^{(k)}, \mathcal{X}_{g_i,t}^{(k)}, \mathcal{Y}_{g_i,t}^{(k)}\}_{t=\{\text{LF},\text{HF}\}}$ and $\{\mathbf{s}^{(k)}, \mathbf{Z}_{\text{MPTP},i}^{(k)}\}$
 Run: Solve Eq. (2) ▷ See Algorithm 2
 Outputs: $\{\mathbf{d}_*^{(k)}, \mathbf{p}_*^{(k)}\}$ and $\{\mathcal{X}_{f,t}^{(k)}, \mathcal{Y}_{f,t}^{(k)}, \mathcal{X}_{g_i,t}^{(k)}, \mathcal{Y}_{g_i,t}^{(k)}\}_{t=\{\text{LF},\text{HF}\}}$ updated
 ### RA phase
 for $i = 1, \dots, n_g$ **do**
 Inputs: $\{\mathcal{X}_{g_i,t}^{(k)}, \mathcal{Y}_{g_i,t}^{(k)}\}_{t=\{\text{LF},\text{HF}\}}$ and $\{\mathbf{d}_*^{(k)}, \mathbf{p}_*^{(k)}\}$
 Run: Solve Eq. (3) ▷ See Algorithm 3
 Outputs: $\{\mathbf{X}_{\text{MPTP},i}^{(k)}, \mathbf{Z}_{\text{MPTP},i}^{(k)}\}$ and $\{\mathcal{X}_{g_i,t}^{(k)}, \mathcal{Y}_{g_i,t}^{(k)}\}_{t=\{\text{LF},\text{HF}\}}$ updated
 $\mathbf{s}_i^{(k+1)} \leftarrow \mathbf{p}_*^{(k)} - \mathbf{X}_{\text{MPTP}}^{(k)}$
 end for
 $k \leftarrow k + 1$
end while

$$t_{\text{DO}}^{\text{new}} = \arg \max_{t \in \{1, \dots, n_t\}} \frac{\sigma_{\text{red},f}^2(t, \mathbf{q}_{\text{DO}}^{\text{new}})}{\text{cost}_{\text{total}}(t)^2} \quad (18)$$

where $\sigma_{\text{red},f}^2(t, \cdot)$ denotes the variance reduction of the surrogate model of the objective function $f(\cdot)$ if the selected point $\mathbf{q}_{\text{DO}}^{\text{new}}$ is added to the fidelity t , and $\text{cost}_{\text{total}}(t)$ denotes the total cost due to the objective function $f(\cdot)$ and constraint functions $g_i(\cdot)$ if the selected point is added to the fidelity t .

Algorithm 2 presents a pseudo-algorithm of the DO stage solved by multi-fidelity BO, where $\mathbf{q}_{\text{DO,AS}}^{\text{new}} = \left\{ \mathbf{d}, \mathbf{p} - \mathbf{s}_i^{(k)}, \mathbf{Z}_{\text{MPTP},i}^{(k)} \right\}_{\text{DO}}^{\text{new}}$ denotes the shifted point in the augmented space corresponding to $\mathbf{q}_{\text{DO}}^{\text{new}}$. As stated above, the new data point is always added (*i.e.*, at each iteration) to the lower-fidelity DoE of $f(\cdot)$ and $g_i(\cdot)$ because of the choice of the sequential training for the AR1 model.

For this optimization problem as well as for the next one, the stopping criterion is the same. It is based on the distance between two successive new points added. Specifically, the stopping criterion is met whenever two consecutive new points proposed by the enrichment criterion are within a defined vicinity. Then the algorithm has converged and the solution is the last selected point.

Algorithm 2 Multi-fidelity BO for DO

Require: $\{\mathcal{X}_{f,t}^{(k)}, \mathcal{Y}_{f,t}^{(k)}, \mathcal{X}_{g_i,t}^{(k)}, \mathcal{Y}_{g_i,t}^{(k)}\}_{t=\{LF, HF\}}$ and $\{\mathbf{s}^{(k)}, \mathbf{Z}_{\text{MPTP},i}^{(k)}\}$ (for $i = 1, \dots, n_g$)

Ensure: $\{\mathbf{d}_*^{(k)}, \mathbf{p}_*^{(k)}\}$ and $\{\mathcal{X}_{f,t}^{(k)}, \mathcal{Y}_{f,t}^{(k)}, \mathcal{X}_{g_i,t}^{(k)}, \mathcal{Y}_{g_i,t}^{(k)}\}_{t=\{LF, HF\}}$ updated

while (stopping criterion not reached) **do**

Construct multi-fidelity surrogates of $f(\cdot)$ and $g_i(\cdot)$

$\mathbf{q}_{\text{DO}}^{\text{new}} \leftarrow$ Solve Eq. (17)

$t_{\text{DO}}^{\text{new}} \leftarrow$ Solve Eq. (18)

$\mathcal{X}_{f,LF}^{(k)} \leftarrow \mathcal{X}_{f,LF}^{(k)} \cup \{\mathbf{q}_{\text{DO}}^{\text{new}}\}$ and $\mathcal{Y}_{f,LF}^{(k)} \leftarrow \mathcal{Y}_{f,LF}^{(k)} \cup \{f^{LF}(\mathbf{q}_{\text{DO}}^{\text{new}})\}$

$\mathcal{X}_{g_i,LF}^{(k)} \leftarrow \mathcal{X}_{g_i,LF}^{(k)} \cup \{\mathbf{q}_{\text{DO,AS}}^{\text{new}}\}$ and $\mathcal{Y}_{g_i,LF}^{(k)} \leftarrow \mathcal{Y}_{g_i,LF}^{(k)} \cup \{g_i^{LF}(\mathbf{q}_{\text{DO,AS}}^{\text{new}})\}$

if $t_{\text{DO}}^{\text{new}} = \text{'HF'}$ **then**

$\mathcal{X}_{f,HF}^{(k)} \leftarrow \mathcal{X}_{f,HF}^{(k)} \cup \{\mathbf{q}_{\text{DO}}^{\text{new}}\}$ and $\mathcal{Y}_{f,HF}^{(k)} \leftarrow \mathcal{Y}_{f,HF}^{(k)} \cup \{f^{HF}(\mathbf{q}_{\text{DO}}^{\text{new}})\}$

$\mathcal{X}_{g_i,HF}^{(k)} \leftarrow \mathcal{X}_{g_i,HF}^{(k)} \cup \{\mathbf{q}_{\text{DO,AS}}^{\text{new}}\}$ and $\mathcal{Y}_{g_i,HF}^{(k)} \leftarrow \mathcal{Y}_{g_i,HF}^{(k)} \cup \{g_i^{HF}(\mathbf{q}_{\text{DO,AS}}^{\text{new}})\}$

end if

Update the surrogates of $f(\cdot)$ and $g_i(\cdot)$

end while

3.3 Multi-fidelity Bayesian Optimization for Reliability Assessment

The second step of SORA is the reliability assessment. It is solved for each constraint by a multi-fidelity BO approach using the surrogate model of $g_i(\cdot)$. Working in the augmented space allows to inherit from a surrogate that already contains information from previous SORA iterations, through the multi-fidelity DoE $\{\mathcal{X}_{g_i,t}^{(k)}, \mathcal{Y}_{g_i,t}^{(k)}\}_{t=\{LF, HF\}}$. The surrogate model of each $g_i(\cdot)$ is then enriched independently, on the "slice" $\mathbf{d}_*^{(k)}$ of the augmented space. The optimization problem Eq. (3) corresponding to the RA phase is solved in a standardized space where the iso-probabilistic transformation is defined by $\mathbf{p}_*^{(k)}$ and \mathbf{Z} . For the sake of clarity on the notations and the functions in the optimization problem, Eq. (3) is recast as

$$\min_{\mathbf{w}} g_i(\mathbf{d}_*^{(k)}, \mathbf{w}) \quad \text{s.t.} \quad \|\mathcal{T}_{\mathbf{p}_*^{(k)}}(\mathbf{w})\| = \beta_i^t, \quad (19)$$

where $\mathbf{w} = \{\mathbf{X}, \mathbf{Z}\}$ is the vector of the random variables in the physical space.

As achieved for DO, the multi-fidelity BO carried out with active learning by selecting new data points to improve the multi-fidelity surrogate model prediction and to find the optimal point corresponding to the MPTP. For each constraint function $g_i(\cdot)$, with $i = 1, \dots, n_g$, the location of the new point $\mathbf{w}_{\text{RA}}^{\text{new}}$ is such that

$$\mathbf{w}_{\text{RA}}^{\text{new}} = \arg \min_{\mathbf{w}} \text{LCB}_{g_i}(n_l, \mathbf{w}) \quad \text{s.t.} \quad \|\mathcal{T}_{\mathbf{p}_*^{(k)}}(\mathbf{w})\| = \beta_i^t \quad (20)$$

where $\text{LCB}_{g_i}(n_l, \mathbf{w})$ denotes the LCB for the high-fidelity ($t = n_l$) surrogate prediction of $g_i(\cdot)$ at point \mathbf{w} . Then, the level of fidelity is selected as presented in Eq. (16):

$$t_{\text{RA}}^{\text{new}} = \arg \max_{t \in \{1, \dots, n_l\}} \frac{\sigma_{\text{red},g_i}^2(t, \mathbf{w}_{\text{RA}}^{\text{new}})}{\text{cost}_{\text{total}}(t)^2} \quad (21)$$

where $\sigma_{\text{red},g_i}^2(t, \cdot)$ and $\text{cost}_{\text{total}}(t)$ respectively denote the reduction of variance for the GP of $g_i(\cdot)$ and the total cost due to the evaluation of $g_i(\cdot)$ when the selected point is added to the fidelity t .

The lay out of the RA block solved with multi-fidelity BO is presented in Algorithm 3, where $\mathbf{w}_{\text{RA,AS}}^{\text{new}} = \{\mathbf{d}_*^{(k)}, \mathbf{X}, \mathbf{Z}\}_{\text{RA}}^{\text{new}}$ is the point in the augmented space corresponding to $\mathbf{w}_{\text{RA}}^{\text{new}}$.

Algorithm 3 Multi-fidelity BO for RA

Require: $\{\mathcal{X}_{g_i,t}^{(k)}, \mathcal{Y}_{g_i,t}^{(k)}\}_{t=\{\text{LF, HF}\}}$ and $\{\mathbf{d}_*^{(k)}, \mathbf{p}_*^{(k)}\}$
Ensure: $\{\mathbf{X}_{\text{MPTP},i}^{(k)}, \mathbf{Z}_{\text{MPTP},i}^{(k)}\}$ and $\{\mathcal{X}_{g_i,t}^{(k)}, \mathcal{Y}_{g_i,t}^{(k)}\}_{t=\{\text{LF, HF}\}}$ updated
while (stopping criterion not reached) **do**
 Construct surrogate of $g_i(\cdot)$
 $\mathbf{w}_{\text{RA}}^{\text{new}} \leftarrow$ Solve Eq. (20)
 $t_{\text{RA}}^{\text{new}} \leftarrow$ Solve Eq. (21)
 $\mathcal{X}_{g_i,\text{LF}}^{(k)} \leftarrow \mathcal{X}_{g_i,\text{LF}}^{(k)} \cup \{\mathbf{w}_{\text{RA,AS}}^{\text{new}}\}$ and $\mathcal{Y}_{g_i,\text{LF}}^{(k)} \leftarrow \mathcal{Y}_{g_i,\text{LF}}^{(k)} \cup \{g_i^{\text{LF}}(\mathbf{w}_{\text{RA,AS}}^{\text{new}})\}$
 if $t_{\text{RA}}^{\text{new}} = \text{'HF'}$ **then**
 $\mathcal{X}_{g_i,\text{HF}}^{(k)} \leftarrow \mathcal{X}_{g_i,\text{HF}}^{(k)} \cup \{\mathbf{w}_{\text{RA,AS}}^{\text{new}}\}$ and $\mathcal{Y}_{g_i,\text{HF}}^{(k)} \leftarrow \mathcal{Y}_{g_i,\text{HF}}^{(k)} \cup \{g_i^{\text{HF}}(\mathbf{w}_{\text{RA,AS}}^{\text{new}})\}$
 end if
 Update the surrogate of $g_i(\cdot)$
end while

4 Computational experiments

The proposed RBDO methodology is here applied and assessed on two test cases in terms of computational performance with respect to alternative approaches (SORA and double-loop). The first test case presents with an analytical function while the second test case correspond to the design of a sounding rocket. The RBDO strategies are implemented in Python, using the SMT package [42] (Surrogate Modeling Toolbox) for the construction of the surrogates. In order to evaluate the contributions of each piece of enhancement of SORA, the implementation and assessment are devised in three steps.

First, BO is integrated to SORA to solve the optimization sub-problems. This approach is named *Bay SORA* in the following. The surrogates of the objective function and constraints functions are constructed. The domain of definition for the objective function remains the same along the SORA process, while the domain of definition for each constraint changes at each step of SORA, and for each DO and RA step. Therefore, an initial DoE $\{\mathcal{X}_f, \mathcal{Y}_f\}$ is constructed for the objective function and enriched along the steps of SORA. Whereas at each step of SORA, a surrogate model of each constraint is built from a new DoE $\{\mathcal{X}_{g_i}^{\text{DO}}, \mathcal{Y}_{g_i}^{\text{DO}}\}$ for the DO phase, and $\{\mathcal{X}_{g_i}^{\text{RA}}, \mathcal{Y}_{g_i}^{\text{RA}}\}$ for the RA phase. These DoEs are constructed using a Latin Hypercube Sampling (LHS) in the design space with $3 * (n_d + n_p)$ points for the DO and in the uncertain space with $3 * (n_X + n_Z)$ points for RA.

Next improvement stands in reusing the information of the different surrogate models built along the iterations of SORA process by working in the augmented space. This strategy is denoted as *Bay SORA AS*. For the objective function (similarly to *Bay SORA*), a DoE $\{\mathcal{X}_f, \mathcal{Y}_f\}$ of $3 * (n_d + n_p)$ is generated in the design space at the beginning of SORA and then enriched along the steps of SORA. For each constraint, a DoE $\{\mathcal{X}_{g_i}, \mathcal{Y}_{g_i}\}$ is constructed at the beginning of the SORA process in the augmented space with $3 * (n_d + n_X + n_Z)$ points. This DoE is then enriched in the augmented space with respect to the design variables during the DO (with \mathbf{Z} fixed) and with respect to the uncertain variables during the RA (with \mathbf{d} fixed). Theses DoEs are then transmitted and enriched along the iterations of the SORA process within each new

optimization problem (DO and RA).

Finally, the last improvement stands in integrating the multi-fidelity approach in the construction and enrichment of the surrogate models in the augmented space. It is the proposed approach of this article is denoted as *MFB-SORA*.

The multi-fidelity DoEs, (as in *Bay SORA AS*), are constructed respectively in the design space and in the augmented space, and enriched along the SORA process. The multi-fidelity DoE $\{\mathcal{X}_{f,\text{LF}}, \mathcal{X}_{f,\text{HF}}, \mathcal{Y}_{f,\text{LF}}, \mathcal{Y}_{f,\text{HF}}\}$ is generated by LHS with the same $3 * (n_d + n_p)$ in each fidelity for the objective function. The multi-fidelity DoE $\{\mathcal{X}_{g_i,\text{LF}}, \mathcal{X}_{g_i,\text{HF}}, \mathcal{Y}_{g_i,\text{LF}}, \mathcal{Y}_{g_i,\text{HF}}\}$ is generated by LHS with the same $3 * (n_d + n_X + n_Z)$ for each fidelity, for each constraint function. In order to respect the necessary condition of nested DoEs for the AR1 training strategy, the multi-fidelity DoEs are nested and during the optimization process, a point added in high-fidelity is automatically added to the low-fidelity model.

Each enhanced version of SORA (*Bay SORA*, *Bay SORA AS* and *MFB-SORA*) is implemented on both test cases and compared to the classical SORA technique. For the analytical test case, a two-level RBDO approach using a Monte-Carlo approach RA step is also implemented. It should be noted that currently, only one repetition of each method is performed on each test case. The evaluation of the robustness of the convergence with respect to the initial choice of DoE will be investigated in further works.

It should be noted that the OpenTurns [43] library was used for the optimization solver. Namely, 'LN_COBYLA' was used for the double-loop approach as well as for the DO and RA optimization problems in the classical SORA approach. Finally, when Bayesian approaches are used, the new computational points for the DoE enrichment are obtained by an 'AUGLAG' approach for DO, and 'LN_COBYLA' for RA. For all the Bayesian optimization problems, the surrogate models of the objective and constraints functions are constructed in a normalized space. For the stopping criterion of the BO processes, one consider that each DO and RA have converged when the distance between two consecutive selected points is less than $5 * 10^{-3}$ in the normalized space.

4.1 Analytical case

The first example consists of a 3-dimensional nonlinear objective function $f(\cdot)$ subjected to two nonlinear probabilistic constraints, such as:

$$\min_{d_0, p_0, p_1} f(d_0, p_0, p_1) \quad \text{s.t.} \quad \begin{cases} \mathbb{P}[g_i(d_0, \mathbf{X}(p_0, p_1), Z_0) \leq 0] \leq P_{f,i}^t & \text{for } i = 1, 2 \\ -0.5 \leq d_0, p_0, p_1 \leq 2.5 \end{cases}$$

where $\mathbf{X} = [X_0, X_1]$ is a random vector of two independent Gaussian variables such that $X_0 \sim \mathcal{N}(p_0, 0.2)$ and $X_1 \sim \mathcal{N}(p_1, 0.2)$ and Z_0 is a random variable such that $Z_0 \sim \mathcal{N}(5, 0.4)$. The target probability of failure is set for each constraints to $P_{f,1}^t = P_{f,2}^t = 0.01$. Two fidelity models (LF and HF) of each function $f(\cdot)$ and $g_i(\cdot)$ are considered. They are denoted as $\{f_{\text{LF}}(\cdot), f_{\text{HF}}(\cdot)\}$ and $\{g_{i,\text{LF}}(\cdot), g_{i,\text{HF}}(\cdot)\}_{i=1,2}$, and are defined such that:

$$\bullet \begin{cases} f_{\text{HF}}(d_0, p_0, p_1) = 2 + (p_0 - 1.5)^2 + (1.2 - p_1 * d_0)^2 + 2 * (d_0 - 1.8)^2 \\ f_{\text{LF}}(d_0, p_0, p_1) = 0.5 * f_{\text{HF}}(d_0, p_0, p_1) + 2 * p_0 - (1.2 - p_1 * d_0)^2 \end{cases}$$

$$\bullet \begin{cases} g_{1,\text{HF}}(d_0, \mathbf{X}(p_0, p_1), Z_0) = 1.0 - d_0 * (X_0 + 1) + (\sqrt{Z_0} + 2) + X_1 - 1.5 \\ g_{1,\text{LF}}(d_0, \mathbf{X}(p_0, p_1), Z_0) = 2.5 * g_{1,\text{HF}}(d_0, \mathbf{X}(p_0, p_1), Z_0) - d_0 * (X_1 + 1) \end{cases}$$

$$\bullet \begin{cases} g_{2,\text{HF}}(d_0, \mathbf{X}(p_0, p_1), Z_0) = 0.2 * (1 + d_0)^2 + X_1 - Z_0 + 2.5 \\ g_{2,\text{LF}}(d_0, \mathbf{X}(p_0, p_1), Z_0) = 0.2 * g_{2,\text{HF}}(d_0, \mathbf{X}(p_0, p_1), Z_0) + 1 + d_0 - Z_0 \end{cases}$$

For each function, it is assumed that the low-fidelity model is 10 times cheaper to evaluate than the high-fidelity one. We set $c_{\text{LF}} = 0.1$ and $c_{\text{HF}} = 1$. Table 1 presents the optimal solutions obtained for each compared methods (two-level RBDO, traditional SORA and the three modified SORA approaches). Moreover, Table 1 provides the optimal objective function value and the constraint values at the optimum. The optimal point is denoted as \mathbf{x}^{opt} . Table 2 compares the computational cost (in terms of number of LF and HF model evaluations) of the modified SORA approach after adding each presented contribution. The cost calculated in the last column presents the total number of exact function calls. For the last row (the multi-fidelity method), the total cost is evaluated by weighting the number of calls to each fidelity by its associated calculation cost, such as $c_{\text{total}} = n_{\text{LF}} * c_{\text{LF}} + n_{\text{HF}} * c_{\text{HF}}$.

Table 1: Optimum obtained by each method for the analytical test case.

	$\mathbf{x}^{\text{opt}} = [d_0, p_0, p_1]^{\text{opt}}$	$f_{\text{HF}}(\mathbf{x}^{\text{opt}})$	$P_{f,1}(\mathbf{x}^{\text{opt}})$	$P_{f,2}(\mathbf{x}^{\text{opt}})$
Two-level approach	[2.5, 0.42, 1.09]	6.47	0.01	0.01
SORA	[2.5, 0.42, 1.09]	6.47	0.01	0.01
Bay SORA	[2.5, 0.42, 1.09]	6.47	0.01	0.01
Bay SORA AS	[2.5, 0.42, 1.09]	6.47	0.01	0.01
MFB-SORA	[2.5, 0.42, 1.09]	6.47	0.01	0.01

All the methods provide the same optimum, regarding the location of \mathbf{x}^{opt} and the corresponding objective function value. This solution is feasible since the probability of failure of each constraint is equal to the limit value $P_{f,i}^t$.

All methods providing the same solution, let us compare the computational costs of each method. The last column gives the total cost in terms of equivalent number of HF model evaluations. The double-loop approach combined with Monte Carlo simulation is expensive in terms of number of HF model evaluations. Considering the modified versions of SORA, regarding the computational cost, each improvement of SORA provides a reduction in the number of calls to the HF model. The integration of BO (*Bay SORA*) divides this total calculation cost by about five times. Indeed, Bayesian approaches have the advantage of being able to solve global optimization problems with a limited number of evaluations of the exact models which is interesting in a computationally intensive context. Then, the construction of surrogate models in the augmented space (*Bay SORA AS*) provides even better results: the computational cost is then divided by more than eleven compared to the classical SORA method. This result is interesting since only by reusing the surrogate information acquired in the previous SORA iterations, the surrogate-based SORA method improves by a factor two its efficiency. The last contribution by adding a low-fidelity model (*MFB-SORA*) and the construction of multi-fidelity surrogate models finally allows to further improve the efficiency of the modified SORA method. The corresponding total cost of this method is $c_{\text{total}} = 117 * 0.1 + 58 = 69.7$. This cost is therefore 23 times smaller than the classical SORA method. These first analyses need to be confirmed

Table 2: Comparison of the computation cost of the proposed method for the analytical test case.

	Number of evaluations of $f_{\text{HF}}(\cdot)$	Number of evaluations of $g_{1,\text{HF}}(\cdot)$	Number of evaluations of $g_{2,\text{HF}}(\cdot)$	Total Cost
Two-level approach	123	$\sim 1.2 \times 10^7$	$\sim 1.1 \times 10^7$	$\sim 2.3 \times 10^7$
SORA	248	624	722	1594
Bay SORA	50	141	141	332
Bay SORA AS	37	49	50	136
MFB-SORA	32 LF 19 HF	43 LF 19 HF	42 LF 20 HF	117 LF 58 HF

on a more complex test case. For that, in the next section, a sounding rocket design problem is considered.

4.2 Sounding Rocket case

The physical test case deals with an optimization problem of a single-stage sounding rocket. Sounding rockets are suborbital launch vehicles that are often used to carry out scientific experiments to study the atmosphere. These rockets perform a first powered phase using either one or multiple stages, then a complete ballistic flight to reach their apogee. Finally, a reentry phase is achieved until landing in the ground or in the sea (Figure 4).

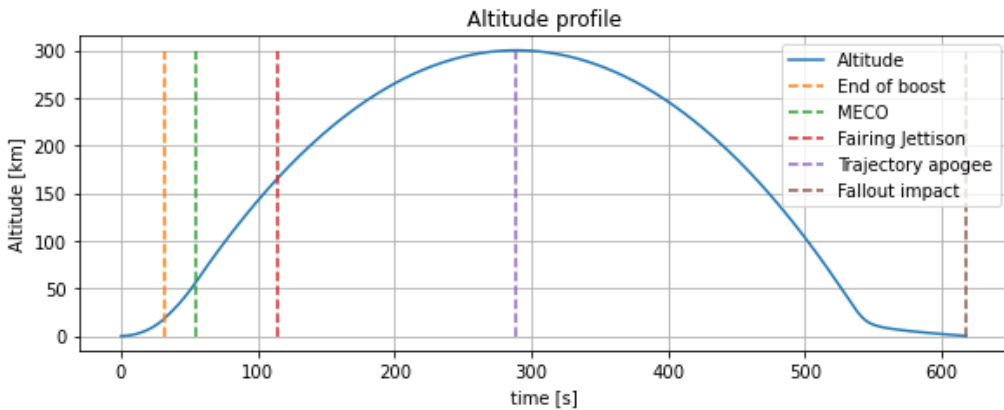


Figure 4: Sounding rocket trajectory (MECO: Main Engine Cut-Off)

In this test case, a RBDO problem of a single-stage solid propellant sounding rocket is carried out (Figure 5). This test case involves a multidisciplinary process involving several disciplines such as trajectory, aerodynamics, structure and propulsion (Figure 6).

These disciplines interact together and the overall design process is implemented using

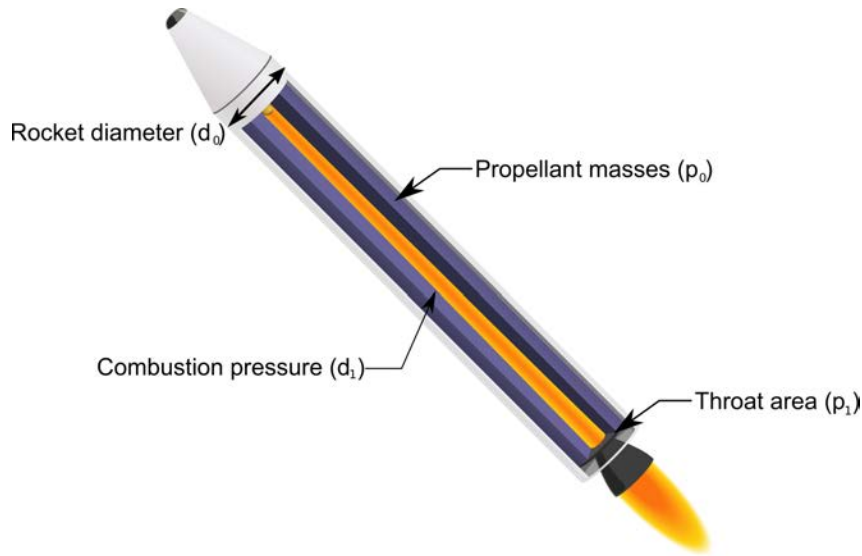


Figure 5: Illustration of solid propellant single stage sounding rocket with the different design parameters (**d** and **p**)

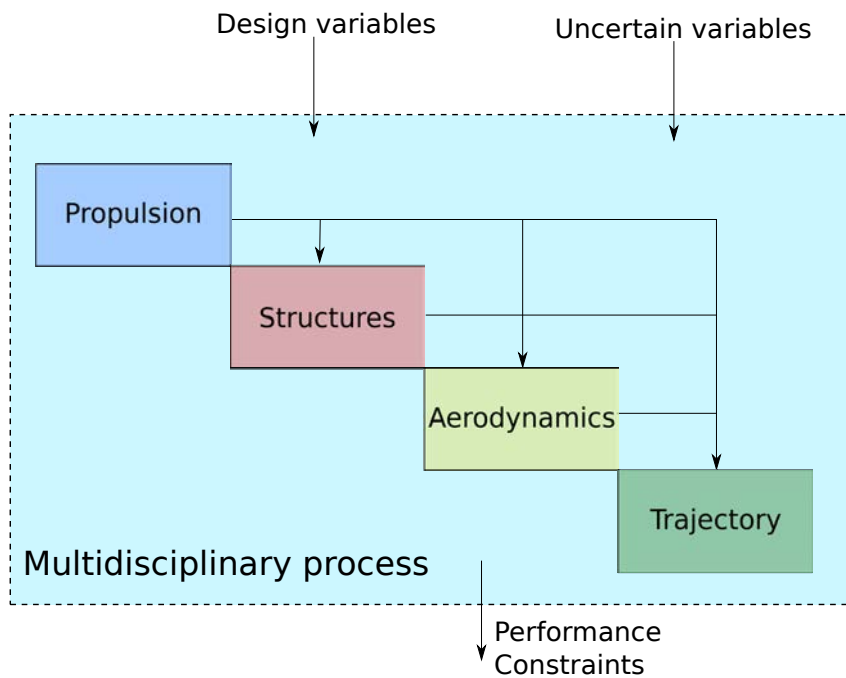


Figure 6: Illustration of the multidisciplinary process of the sounding rocket test case

OpenMDAO [44]. Two fidelity levels are involved, depending on simplifications in the disciplines relative to the aerodynamics and structure. It is assessed that the computational cost of the low fidelity model is ten times lower than the high fidelity: $c_{LF} = 0.1$ and $c_{HF} = 1$.

In order to collect data or perform experiments at a given altitude Alt_{apogee}^t , it is crucial to ensure with a high level of confidence the probability of reaching this target altitude at the apogee. The RBDO problem consists in minimizing the Gross Lift-Off Weight (GLOW) while ensuring to reach a target altitude at apogee.

An illustration of single-stage sounding rocket trajectory is given in Figure 4, with an altitude at apogee of 300 km. During the trajectory, the fairing of the sounding rocket is jettisoned in order for the payload to perform the experimentation. The corresponding optimization problem can be formulated such as:

$$\begin{aligned} & \min_{d_0, d_1, p_0, p_1} \text{GLOW}(d_0, d_1, p_0, p_1) \\ \text{s.t. } & \mathbb{P} [\text{Alt}(d_0, d_1, \mathbf{X}(p_0, p_1), Z_0) \leq \text{Alt}_{\text{apogee}}^t] \leq P_f^t \end{aligned}$$

where:

- d_0 is the stage diameter (m), with $0.2 \leq d_0 \leq 0.6$,
- d_1 is the combustion chamber pressure (MPa) for the solid rocket propulsion, with $9 \leq d_1 \leq 11$,
- p_0 is the propellant mass (kg), with $350 \leq p_0 \leq 500$,
- p_1 is the throat area (m²) of the nozzle for the solid rocket engine, with $1 * 10^{-3} \leq p_1 \leq 2.5 * 10^{-3}$,
- Z_0 is the uncertainty on drag parameter for the aerodynamics modeling during ascent phase.

The parameters $\{d_0, d_1, p_0, p_1\}$ are the design variables. $\mathbf{X} = [X_0, X_1]$ and Z_0 are the random variables such that $X_0 \sim \mathcal{N}(p_0, 0.1)$, $X_1 \sim \mathcal{N}(p_1, 0.25)$ and $Z_0 \sim \mathcal{N}(0, 0.1)$. The random vector \mathbf{X} models uncertainty due to the manufacturing process of the sounding rocket (for the throat area of the rocket engine) and the fueling operation before the launch. Moreover, Z_0 characterizes the uncertainty on the modeling of drag during ascent phase. Due to these different uncertainties, the sounding rocket has different trajectories. Two multidisciplinary processes are considered in this test case a LF and a HF process with differences regarding the aerodynamics and the structure disciplines. For the structure, the low fidelity models involves a statistical relationship between the inert mass as a function of the propellant mass whereas the high fidelity model computes the masses of all the elements (nose cone, equipment bay, nozzle, engine, *etc.*) of the stage). Considering the aerodynamics discipline, low fidelity models are calibrated with respect to expert knowledge whereas for high fidelity models, an early design aerodynamics code (MISSILE [45]) is used.

Figure 7 shows the dispersion of the trajectories (using the Low-Fidelity and the High-Fidelity models), over 50 realizations of the aleatory variables, of the sounding rocket and the comparison between its maximum altitude and the threshold to reach. In Figure 7, two different sets of trajectories are shown: one computed with the HF code and one with the LF code. These two fidelity models leads to similar trajectories by with some discrepancies due to the simplifications in the low fidelity models of the aerodynamics and the structures.

The objective of the design study is to optimize GLOW with respect to the design parameters of the sounding rocket while ensuring that the probability of not reaching the target altitude (in red in Figure 7) is less than a certain probability of failure. This target probability of failure is set to $P_f^t = 0.001$. The different fidelities of each functions are denoted $\{f_{\text{LF}}(\cdot), f_{\text{HF}}(\cdot)\}$ and $\{g_{\text{LF}}(\cdot), g_{\text{HF}}(\cdot)\}$.

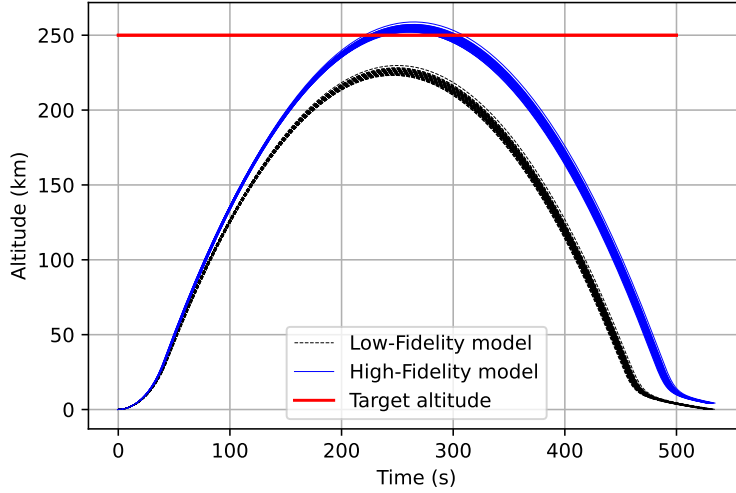


Figure 7: Dispersion of trajectories of the sounding rocket due to uncertainties, computed with the HF code and the LF code

Table 3 presents the optimal solution and its corresponding objective and constraint value given by each compared method (SORA, Bay SORA, Bay SORA AS and MFB-SORA). The optimal point is denoted as \mathbf{x}^{opt} . Table 4 compares the computational cost of each method. The costs calculated in the last column are computed as for the analytical case.

Table 3: Optimum obtained by each method for the sounding rocket test case.

	$\mathbf{x}^{\text{opt}} = [d_0, d_1, p_0, p_1]^{\text{opt}}$	$f_{\text{HF}}(\mathbf{x}^{\text{opt}})$	$P_{f,1}(\mathbf{x}^{\text{opt}})$
SORA	[51.1, 97.5, 43.8, 14.8]	683.47	0.001
Bay SORA	[51.1, 97.4, 43.8, 14.8]	683.47	0.001
Bay SORA AS	[51.0, 98.1, 43.8, 14.7]	683.47	0.001
MFB-SORA	[51.0, 97.0, 43.8, 14.9]	683.47	0.001

For this physical case, all the methods provide similar results for optimum (with some small differences regarding the location of \mathbf{x}^{opt}). Some of the components of \mathbf{x}^{opt} vary a bit depending on the methods used. This variation is explained by the fact that the solution of the problem is on a plateau, and thus several combinations of input parameters provide the same objective function value. Indeed, all solutions provide the same objective function value, and are feasible with respect to the probabilistic constraint. The value of $P_{f,1}$ at the optimal point (\mathbf{x}^{opt}) is equal to the limit value P_f^t .

Let us compare the corresponding computational costs of each method. In this case, the double-loop method could not be tested, due to the computational cost of the codes used (impossibility to carry out a number of multidisciplinary process evaluations in the magnitude of 10^7). As for the first case, the computational cost of the standard SORA approach is compared to the various SORA improvements. Each improvement of SORA provides a reduction in the

Table 4: Comparison of the computation cost of the proposed method for the sounding rocket test case.

	Number of evaluations	Number of evaluations	Total Cost
	of $f_{\text{HF}}(\cdot)$	of $g_{\text{HF}}(\cdot)$	
SORA	1773	2281	4054
Bay SORA	133	253	386
Bay SORA AS	105	122	227
MFB-SORA	82 LF	103 LF	185 LF
	31 HF	35 HF	66 HF

number of evaluations of the HF code. *Bay SORA* divides the global computation cost of SORA by about ten times, by integrating Bayesian optimization. This result is very promising since it shows the interest of using surrogate models to reduce the computation time, especially in the case of complex systems. Then, the construction of surrogate models in the augmented space improves the efficiency: the cost of *Bay SORA AS* method is 18 times lower than the classical SORA. The idea of reusing the surrogate information acquired allows to reduce the cost as well as for the analytical case. Finally, using the information provided by a lower fidelity model with the proposed *MFB-SORA* approach, total cost is reduced by about 48 times ($c_{\text{total}} = 185 * 0.1 + 66 = 84.5$). Each contribution improves the efficiency of the classical SORA method.

5 Conclusions

In the present work focused on Reliability-Based Design Optimization (RBDO), extensions of the Sequential Optimization and Reliability Assessment (SORA) have been proposed. SORA approach is an efficient alternative to two-level formulations of RBDO problems decoupling optimization from reliability analysis and transforming the process into a sequence of deterministic optimization problem and reliability analysis problem. Moreover, reliability analysis is solved using First Order Reliability Method (FORM) leading to another optimization problem. In the present paper, three different improvements of classical SORA have been proposed. First, the use of Bayesian Optimization using surrogate models in order to solve the optimization problems at each iteration of SORA has been proposed. Second, the idea is to reuse the information of the surrogates learned during the iterations of SORA by constructing these surrogates in an augmented space combining the domain of definition of the random variables and the design variables. Finally, in order to reduce the computational time, the approach has been modified to take into account information from different levels of fidelity, through a multi-fidelity framework. Each of the contributions made to SORA have been tested and compared on two different test cases: an analytical test case and a physical test case involving the design of a sounding rocket under the probabilistic constraint of reaching a certain altitude considering different uncertainties.

Each of the improvements of SORA allowed to obtain the feasible solution for each test case problem. These results were compared to reference results provided by classical methods (classical SORA and two-level approach). Each SORA improvement reduces the number of eval-

uations of the HF simulation code. The integration of Bayesian optimization allows to solve the optimization sub-problems (deterministic optimization and reliability analysis) of SORA with a limited number of exact model evaluations, which is interesting in an intensive computational context. Secondly, the construction of surrogate models in an augmented space allows to even more reduce the costs of calculation. Indeed, just by reusing the information (through the Design of Experiments - DoEs) of the surrogate along the SORA iterations, the number of calls to the HF code during the enrichment of the surrogates are reduced. Indeed, closed to the SORA convergence, the solved optimization sub-problems are similar to the previous SORA iteration. As a result, the transmission of information learned during iterations allows the following optimization sub-problems to be solved with fewer and fewer HF code evaluations as the surrogate models are already accurate. Finally, the MFB-SORA method presented in this article proposes to use information from different levels of fidelity by constructing multi-fidelity surrogate models in this augmented space. The first analyses presented in this paper have shown that the proposed MFB-SORA method drastically reduces calculation costs, which presents a real advantage in a context of complex systems where calculation costs are expensive.

Future works will investigate the robustness of the method according to the initial DoEs. Repetitions of each method will be performed considering different initial DoEs. In addition, different criteria for multi-fidelity enrichment will be compared. Another way of improvement of the proposed method would be to consider other multi-fidelity surrogate models than Auto-Regressive 1 (AR1), where the robustness of MFB-SORA could be confronted to test cases presenting non-linear dependencies between fidelity models.

6 Acknowledgments

The authors thank M. Glen Sire (ONERA) for the development of the sounding rocket test case. This work is supported by a PhD thesis funded by ONERA and CERFACS.

REFERENCES

- [1] J. Tu, K. Choi, and P. Y.H., “A new study on reliability-based design optimization,” Journal of Mechanical Design, vol. 121, no. 4, pp. 557–564, 1999.
- [2] J. Liang, Z. P. Mourelatos, and J. Tu, “A single-loop method for reliability-based design optimization,” in International design engineering technical conferences and computers and information in engineering conference, vol. 46946, pp. 419–430, 2004.
- [3] X. Du and W. Chen, “Sequential optimization and reliability assessment method for efficient probabilistic design,” Journal of Mechanical Design, vol. 126, no. 2, pp. 225–233, 2004.
- [4] K. Breitung, “Asymptotic approximations for multinormal integrals,” Journal of Engineering Mechanics, vol. 110, no. 3, pp. 357–366, 1984.
- [5] H. R. Maier, B. J. Lence, B. A. Tolson, and R. O. Foschi, “First-order reliability method for estimating reliability, vulnerability, and resilience,” Water Resources Research, vol. 37, no. 3, pp. 779–790, 2001.
- [6] V. Dubourg, B. Sudret, and J.-M. Bourinet, “Reliability-based design optimization using kriging surrogates and subset simulation,” Structural and Multidisciplinary Optimization, vol. 44, no. 5, pp. 673–690, 2011.

-
- [7] M. Moustapha and B. Sudret, “Surrogate-assisted reliability-based design optimization: a survey and a unified modular framework,” Structural and Multidisciplinary Optimization, vol. 60, pp. 2157–2176, 2019.
- [8] M. Moustapha, B. Sudret, J.-M. Bourinet, and B. Guillaume, “Quantile-based optimization under uncertainties using adaptive kriging surrogate models,” Structural and multidisciplinary optimization, vol. 54, pp. 1403–1421, 2016.
- [9] C. E. Rasmussen and C. K. Williams, Gaussian processes for machine learning, vol. 1. Springer, 2006.
- [10] D. R. Jones, M. Schonlau, and W. J. Welch, “Efficient global optimization of expensive black-box functions,” Journal of Global optimization, vol. 13, no. 4, p. 455, 1998.
- [11] P. Goovaerts et al., Geostatistics for natural resources evaluation. Oxford University Press on Demand, 1997.
- [12] C. E. Rasmussen and C. K. Williams, “Gaussian processes in machine learning,” Lecture notes in computer science, vol. 3176, pp. 63–71, 2004.
- [13] S. Au, “Reliability-based design sensitivity by efficient simulation,” Computers & structures, vol. 83, no. 14, pp. 1048–1061, 2005.
- [14] M. A. Alvarez, L. Rosasco, and N. D. Lawrence, “Kernels for vector-valued functions: A review,” Foundations and Trends® in Machine Learning, vol. 4, no. 3, pp. 195–266, 2012.
- [15] M. C. Kennedy and A. O’Hagan, “Predicting the output from a complex computer code when fast approximations are available,” Biometrika, vol. 87, no. 1, pp. 1–13, 2000.
- [16] P. Perdikaris, M. Raissi, A. Damianou, N. D. Lawrence, and G. E. Karniadakis, “Nonlinear information fusion algorithms for data-efficient multi-fidelity modelling,” Proceedings of the Royal Society A: Mathematical, Physical and Engineering Sciences, vol. 473, no. 2198, p. 20160751, 2017.
- [17] L. Brevault, M. Balesdent, and A. Hebbal, “Overview of gaussian process based multi-fidelity techniques with variable relationship between fidelities, application to aerospace systems,” Aerospace Science and Technology, vol. 107, p. 106339, 2020.
- [18] A. Chaudhuri, A. N. Marques, R. Lam, and K. E. Willcox, “Reusing information for multifidelity active learning in reliability-based design optimization,” in AIAA Scitech 2019 Forum, p. 1222, 2019.
- [19] A. Chaudhuri, A. N. Marques, and K. Willcox, “mfegra: Multifidelity efficient global reliability analysis through active learning for failure boundary location,” Structural and Multidisciplinary Optimization, vol. 64, no. 2, pp. 797–811, 2021.
- [20] K. Song, Y. Zhang, X. Zhuang, X. Yu, and B. Song, “Reliability-based design optimization using adaptive surrogate model and importance sampling-based modified sora method,” Engineering with Computers, vol. 37, pp. 1295–1314, 2021.

-
- [21] K. Yoo, O. Bacarreza, and M. F. Aliabadi, “A novel multi-fidelity modelling-based framework for reliability-based design optimisation of composite structures,” Engineering with Computers, pp. 1–14, 2022.
- [22] Y. Aoues and A. Chateaneuf, “Benchmark study of numerical methods for reliability-based design optimization,” Structural and multidisciplinary optimization, vol. 41, no. 2, pp. 277–294, 2010.
- [23] S. Mahadevan, “Monte carlo simulation,” in Reliability-based mechanical design., pp. 123–146, Marcel Dekker Inc., New-York, Basel, Hong Kong, 1997.
- [24] E. Nikolaidis and R. Burdisso, “Reliability based optimization: a safety index approach,” Computers & structures, vol. 28, no. 6, pp. 781–788, 1988.
- [25] J. Ji, C. Zhang, Y. Gao, and J. Kodikara, “Reliability-based design for geotechnical engineering: an inverse form approach for practice,” Computers and Geotechnics, vol. 111, pp. 22–29, 2019.
- [26] H.-C. Wu, “The Karush-Kuhn-Tucker optimality conditions in an optimization problem with interval-valued objective function,” European Journal of operational research, vol. 176, no. 1, pp. 46–59, 2007.
- [27] L. Le Gratiet and J. Garnier, “Recursive co-kriging model for design of computer experiments with multiple levels of fidelity,” International Journal for Uncertainty Quantification, vol. 4, no. 5, 2014.
- [28] J. Močkus, “On Bayesian methods for seeking the extremum,” in Optimization Techniques IFIP Technical Conference: Novosibirsk, July 1–7, 1974, pp. 400–404, Springer, 1975.
- [29] D. R. Jones, “A taxonomy of global optimization methods based on response surfaces,” Journal of Global Optimization, vol. 21, pp. 345–383, 2001.
- [30] A. Žilinskas, “A review of statistical models for global optimization,” Journal of Global Optimization, vol. 2, pp. 145–153, 1992.
- [31] P. Auer, “Using confidence bounds for exploitation-exploration trade-offs,” Journal of Machine Learning Research, vol. 3, no. Nov, pp. 397–422, 2002.
- [32] N. Srinivas, A. Krause, S. M. Kakade, and M. Seeger, “Gaussian process optimization in the bandit setting: No regret and experimental design,” arXiv preprint arXiv:0912.3995, 2009.
- [33] J. M. Parr, A. J. Keane, A. I. Forrester, and C. M. Holden, “Infill sampling criteria for surrogate-based optimization with constraint handling,” Engineering Optimization, vol. 44, no. 10, pp. 1147–1166, 2012.
- [34] C. Audet, J. Denni, D. Moore, A. Booker, and P. Frank, “A surrogate-model-based method for constrained optimization,” in 8th symposium on multidisciplinary analysis and optimization, p. 4891, 2000.

-
- [35] A. Tran, J. Tranchida, T. Wildey, and A. P. Thompson, “Multi-fidelity machine-learning with uncertainty quantification and bayesian optimization for materials design: Application to ternary random alloys,” The Journal of Chemical Physics, vol. 153, no. 7, p. 074705, 2020.
- [36] S. Zhang, W. Lyu, F. Yang, C. Yan, D. Zhou, X. Zeng, and X. Hu, “An efficient multi-fidelity bayesian optimization approach for analog circuit synthesis,” in Proceedings of the 56th Annual Design Automation Conference 2019, pp. 1–6, 2019.
- [37] H. Huang, Z. Liu, H. Zheng, X. Xu, and Y. Duan, “A proportional expected improvement criterion-based multi-fidelity sequential optimization method,” Structural and Multidisciplinary Optimization, vol. 66, no. 2, p. 30, 2023.
- [38] L. Shu, P. Jiang, and Y. Wang, “A multi-fidelity Bayesian optimization approach based on the expected further improvement,” Structural and Multidisciplinary Optimization, vol. 63, pp. 1709–1719, 2021.
- [39] S. Takeno, H. Fukuoka, Y. Tsukada, T. Koyama, M. Shiga, I. Takeuchi, and M. Karasuyama, “Multi-fidelity Bayesian optimization with max-value entropy search and its parallelization,” in International Conference on Machine Learning, pp. 9334–9345, PMLR, 2020.
- [40] K. Kandasamy, G. Dasarathy, J. Oliva, J. Schneider, and B. Póczos, “Multi-fidelity gaussian process bandit optimisation,” Journal of Artificial Intelligence Research, vol. 66, pp. 151–196, 2019.
- [41] M. Meliani, N. Bartoli, T. Lefebvre, M.-A. Bouhlef, J. R. Martins, and J. Morlier, “Multi-fidelity efficient global optimization: Methodology and application to airfoil shape design,” in AIAA aviation 2019 forum, p. 3236, 2019.
- [42] M. A. Bouhlef, J. T. Hwang, N. Bartoli, R. Lafage, J. Morlier, and J. R. Martins, “A python surrogate modeling framework with derivatives,” Advances in Engineering Software, vol. 135, p. 102662, 2019.
- [43] M. Baudin, A. Dutfoy, B. Iooss, and A.-L. Popelin, “OpenTURNS: an industrial software for uncertainty quantification in simulation,” in Handbook of uncertainty quantification, pp. 2001–2038, Springer, 2017.
- [44] J. S. Gray, J. T. Hwang, J. R. R. A. Martins, K. T. Moore, and B. A. Naylor, “OpenM-DAO: An open-source framework for multidisciplinary design, analysis, and optimization,” Structural and Multidisciplinary Optimization, vol. 59, pp. 1075–1104, April 2019.
- [45] P. Denis, “Onera’s aerodynamic prediction code- missile,” in RTO/AGARD, Symposium on Missile Aerodynamics, Sorrento, Italy, May 11-14, 1998, ONERA, TP, no. 1998-56, 1998.